

VERSION: MARCH 17, 2017

Typeset using L^AT_EX **modern** style in AASTeX61

THE WISCONSIN H-ALPHA MAPPER SKY SURVEY DATA RELEASE DOCUMENTATION

L. MATTHEW HAFFNER^{1,2}

¹*University of Wisconsin—Madison*

²*Space Science Institute*

ABSTRACT

The Wisconsin H-Alpha Mapper Sky Survey (WHAM-SS) consists of more than 49,000 spectra taken around H α ($-100 \text{ km s}^{-1} \lesssim v_{\text{LSR}} \lesssim +100 \text{ km s}^{-1}$) on a nested grid with approximately 1° resolution that covers the whole sky. At the time of writing, it is the most sensitive spectrally resolved survey of H α from the Milky Way. Emission from the Galaxy is detected in every pointing of the survey. The northern portion of the survey (NSS; $\delta \geq -30^\circ$) was released in 2001. In 2009, we moved WHAM to Cerro Tololo in Chile to observe the southern sky (SSS) and complete this all-sky H α survey. This document accompanies the data release to provide guidance for users. More technical details on the WHAM facility, survey strategy, reduction methodology, and science can be found through the included references.



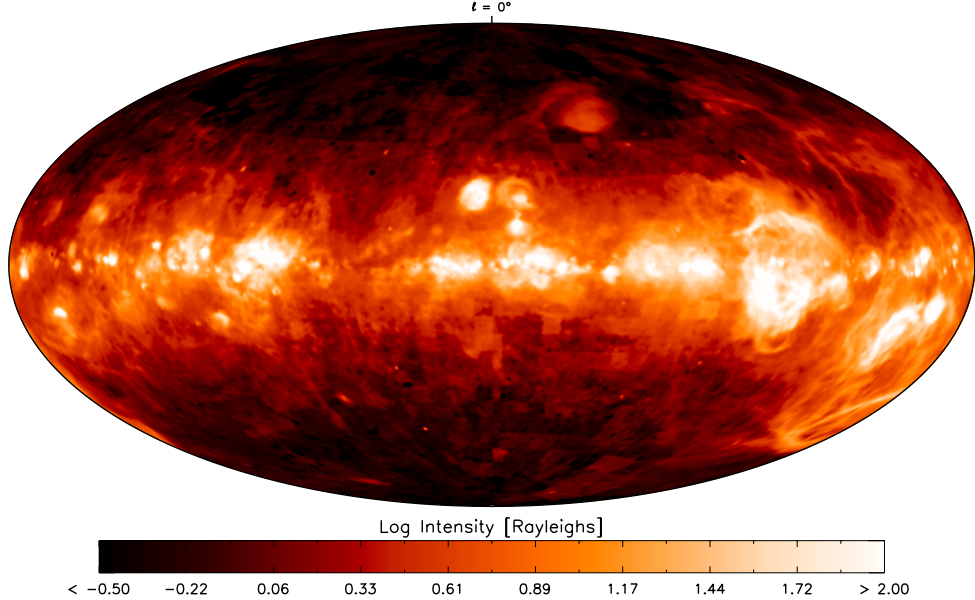


Figure 1. WHAM Sky Survey. A Hammer-Aitoff projection in Galactic coordinates of the WHAM-SS with the Galactic Center at the center of the projection. The logarithm of integrated intensity ($-100 \text{ km s}^{-1} < v_{\text{LSR}} < 100 \text{ km s}^{-1}$) in Rayleighs is represented by the color-scaled image. Some of the dynamic range of the survey is clipped ($I_{\text{H}\alpha}^{\text{max}} = 100 \text{ R}$) to highlight fainter diffuse ionized structures.

1. INTRODUCTION

The WHAM-SS (Fig. 1) is available for public download at <http://www.astro.wisc.edu/wham/>. WHAM was built and has been supported through funds from the National Science Foundation since 1992. Use of the data is open to all researchers; however, *it is important to properly attribute all use of this data*. As of the writing of this document, the all-sky survey paper is still being prepared for submission:

Haffner, Reynolds, Madsen, Babler, Tufte, Hill, Barger, Jaehnig, Mierkiewicz, Percival, Chopra, Pingel, Reese, & Wunderlin 2017, in preparation.

Until this work is accepted, a concise reference for the new southern data is:

Haffner, Reynolds, Madsen, Hill, Barger, Jaehnig, Mierkiewicz, Percival, & Chopra 2010 *Early Results from the Wisconsin H-Alpha Mapper Southern Sky Survey*, in ASP Conf. Ser., Vol. 438, “The Dynamic Interstellar Medium: A Celebration of the Canadian Galactic Plane Survey”, ed. R. Kothes, T. L. Landecker, & A. G. Willis, 388.

Consult the Northern Sky Survey (NSS) release publication for full details of the facility, survey strategy, and reduction methods:

Haffner, Reynolds, Tufte, Madsen, Jaehnig, & Percival 2003 *The Wisconsin H α Mapper Northern Sky Survey*, ApJS, 149, 405.

More technical background on the WHAM instrument and facility can be found in these references:

Tufte, S. L. *The WHAM Spectrometer: Design, Performance Characteristics, and First Results*, 1997, PhD Thesis, University of Wisconsin—Madison.

Haffner, L. M. *The Warm Ionized Medium: Distribution, Kinematics, and Physical Conditions*, 1999, PhD Thesis, University of Wisconsin—Madison.

Finally, when using this data, please add an acknowledgment to the effect of:

The Wisconsin H-Alpha Mapper and its H α Sky Survey have been funded primarily by the National Science Foundation. The facility was designed and built with the help of the University of Wisconsin Graduate School, Physical Sciences Lab, and Space Astronomy Lab. NOAO staff at Kitt Peak and Cerro Tololo provided on-site support for its remote operation.

Please check our website for future reference information, especially before you submit your work for publication. We expect the all-sky survey paper to be submitted in early 2017.

2. RELEASE VERSIONS

Public releases are tagged with a *major label*, a *survey version*, and a *revision date*. The initial release is labeled **DR1**. Version date strings (YYMMDD) match the internal survey base file they have been created from. Changes in the version reflect changes to the fundamental spectra, reduction, or calibration of the survey. The revision date (YYMMDD) marks when the release datasets were created. A change in revision *without* a change in the version denotes a change or fix in the production of the release output files (but not in the survey dataset). Using these designations, the base name for public survey files follows: **wham-ss-LABEL-vVERSION-RELEASE** (e.g., **wham-ss-DR1-v161116-170111** : a file generated on 01/11/2017 from the DR1 survey base version 161116).

Significant future improvement to the WHAM-SS primarily involves changing how the northern and southern surveys are combined to form the all-sky survey. **DR1** simply adds the missing southern pointings to the well-vetted NSS. Current plans for subsequent major releases are as follows:

DR1: All-sky survey created from unmodified NSS ($\delta \gtrsim -30^\circ$) with SSS filling in blocks not observed ($\delta \lesssim -30^\circ$) in the NSS. Multiple (and verified good) observations of SSS pointings are averaged to provide better velocity coverage and potentially higher S/N in some regions. No averaging of the NSS with the SSS in the overlap region ($-30^\circ < \delta < +30^\circ$).

DR2: NSS and SSS overlap blocks ($-30^\circ < \delta < +30^\circ$) are evaluated and averaged whenever possible. In the event of discrepancies, the trends from neighboring regions will be evaluated to determine which survey better represents the emission. For example, NSS regions affected by more serious zodiacal contamination (§4.4) could be replaced by SSS observations.

DR3: Re-reduce any remaining block discontinuities (including older NSS observations) based on decades of reduction experience, what is revealed in the continuous all-sky structure, and how any remaining $H\alpha$ discontinuities compare to structure in other WHAM emission line surveys (e.g., [S II] and [N II]).

3. DATA FORMAT

The WHAM-SS is available from our website in several formats. A velocity integrated ($-80 \text{ km s}^{-1} \leq v_{\text{LSR}} \leq +80 \text{ km s}^{-1}$) version of the survey (§3.1) is distributed as an ASCII table and a FITS binary table. The full kinematic survey (§3.2) is available as a FITS binary table and IDL save file. Our data were taken on an irregular grid optimized for large sky coverage over a short observing time. These two formats preserve the high-quality spectra and spatial sampling most faithfully. However, the survey has been interpolated onto a regular grid and is available as a FITS image (§3.3) and FITS velocity cube (§3.4).

Throughout the datasets, all intensity units are given in Rayleighs. $1 \text{ R} = 10^6/4\pi \text{ photons cm}^{-2} \text{ s}^{-1} \text{ ster}^{-1} = 2.4 \times 10^{-7} \text{ ergs cm}^{-2} \text{ s}^{-1} \text{ ster}^{-1}$; $1 \text{ R} \approx 2.25 \text{ pc cm}^{-6}$ at $T = 8,000 \text{ K}$ in the absence of dust extinction along the line of sight.

3.1. Integrated Survey

Each of the integrated survey distributions contains a short **README** with a summary of the column contents. The following data are included:

GAL-LON, GAL-LAT: The Galactic longitude and latitude (IAU 1958 reference frame) of the pointing in degrees.

INTEN: The $H\alpha$ intensity of the pointing over the integration range $-80 \text{ km s}^{-1} \leq v_{\text{LSR}} \leq +80 \text{ km s}^{-1}$. Note that in certain directions, especially close to the plane toward the inner Galaxy, this range does not fully encompass all Galactic emission. However, it does give a fairly accurate representation of the relative intensity over the whole sky. The majority of pointings contain at least this velocity range (see §4.1 below). As we increase the velocity coverage of the survey, this range will be increased in the future. Units are given in Rayleighs.

ERROR: The calculated error in the $H\alpha$ intensity. This value is derived from the measured error in each contributing spectral data point. No additional error is included due to systematic or calibration uncertainties. If this field is zero, this pointing is potentially contaminated by a bright star and the **INTEN** field of this

pointing has been replaced with an average of nearby neighbors. See the next item for details.

STAR, OINTEN: About 10% of the one-degree beam survey pointings contain a bright star whose spectrum dominates the spectrum. In these directions, the $H\alpha$ emission profile is extremely difficult to isolate and the **STAR** flag is set to 1. For the integrated survey release, we have replaced the **INTEN** value for these pointings by an average of nearby neighbors. The original integrated intensity is provided here as a reference in the **OINTEN** field.

BLOCK, POINTING: WHAM survey observations are organized into groups of spectra called a “block”. Most blocks consist of 30–49 pointings. Within each block, each consecutive pointing exposure is only one degree away from the last, minimizing large changes in the background from spectrum to spectrum. Each block has been numbered and is provided here to help aid in discriminating between real Galactic features and residual systematic effects that can be difficult to fully remove. These effects are typically quite faint and less than 0.1 R. More details can be found in §4.3.

A collection of pre-generated $H\alpha$ maps are also provided on our website in a variety of graphic formats, projection centers, and integration ranges.

3.2. Kinematic Survey

The kinematic survey presents the full WHAM-SS product, the most sensitive resolved Galactic $H\alpha$ emission spectra taken over the whole sky. The fields from the integrated survey are also provided in this release as a convenience. The data provided are:

GAL-LON, GAL-LAT: The Galactic longitude and latitude (IAU 1958 reference frame) of the pointing in degrees.

VELOCITY: The velocity vector of this pointing given as km s^{-1} in the Local Standard of Rest (LSR) reference frame. Survey observations are taken at fixed *geocentric* velocity windows to minimize systematic effects of geocoronal and atmospheric removal. As a result, the actual LSR velocity coverage changes from pointing to pointing (see §4.1 and §5.3). Expanded velocity coverage beyond the nominal 200-km s^{-1} -wide window is available for some of the pointings (see §5.3). Ongoing observations are extending the coverage to at least $-150\text{ km s}^{-1} \lesssim v_{\text{LSR}} \lesssim +150\text{ km s}^{-1}$ as time and funding permits.

DATA: The $H\alpha$ intensity vector of this pointing in $\text{R (km s}^{-1})^{-1}$.

VARIANCE: The variance vector of this pointing in $(\text{R (km s}^{-1})^{-1})^2$.

INTEN, ERROR, STAR, OINTEN, BLOCK, POINTING: See the description of these fields in §3.1 above.

3.3. *FITS Image: Re-gridded Integrated Survey*

Using the INTEN values described in §3.1, we create a regularly gridded version of the Sky Survey using the Natural Neighbor interpolation method. This array is output directly to a FITS primary image with the plate carrée projection (CAR). While the pixel sampling in this image is $0''.25$, keep in mind that the WHAM data are collected with a $1''$ -diameter beam. An error map will be supplied to accompany the intensity image in a later release.

This image can be considered a companion to the three-survey combination release of Finkbeiner (2003). There, higher spatial resolution in many regions is supplied by wide-field imaging surveys (SHASSA, Gaustad et al. 2001; VTSS, Dennison et al. 1998) while the WHAM-NSS provides absolute calibration and fills in over the high-latitude northern sky. Here, the image originates entirely from the WHAM-SS. Since we limit emission between $-80 \text{ km s}^{-1} \leq v_{\text{LSR}} \leq +80 \text{ km s}^{-1}$, some higher velocity features (e.g., the Magellanic Clouds) are not fully present in the WHAM-SS image.

3.4. *FITS Cube: Re-gridded Kinematic Survey*

A regularly gridded representation of the full kinematic survey (§3.2) is also provided. Every spectrum is aligned with a uniform velocity axis before each channel is spatially interpolated onto a regular grid using the same method as used for the integrated FITS image (§3.3). As noted in §3.2 and §4.1 each pointing has a unique, (slightly) non-linear velocity vector. As of this writing, there is no interpolation of the spectra along the velocity axis. The translation of the spectra to a regular output grid creates a small amount of smoothing along the velocity axis of the cube. At $\sim \pm 100 \text{ km s}^{-1}$, the difference between the channel velocity of the cube and the average velocity of the data points that contribute to the channel is $\sim 0.5 \text{ km s}^{-1}$. Since we do not yet have velocity coverage for every channel in every direction (see §5.3), higher-velocity channels have regions of missing data represented by NaN values.

4. NOTES

Full details about our observation strategy and reduction procedures are presented in Haffner et al. (2017, 2003). We highlight some of the important details when working with the data here as well.

4.1. *Velocity*

WHAM-SS spectra are calibrated to the geocentric velocity frame by the geocoronal $\text{H}\alpha$ line present in each observation. Fits to this line result in a velocity registration better than 1 km s^{-1} . As it is excited primarily by solar $\text{Ly}\beta$ and does not contain the full assortment of recombination cascade components, the geocoronal $\text{H}\alpha$ line is offset 2.33 km s^{-1} to the blue of the recombination $\text{H}\alpha$ zero-point. This offset, corrections for the earth’s rotation and orbital motion, and the conventional vector for peculiar solar motion ($v = +20.0 \text{ km s}^{-1}$ toward $\alpha_{1900} = 18$, $\delta_{1900} = +30$) along the line of sight are used to translate the raw velocity frame to the LSR.

WHAM survey data is taken with the spectrometer velocity range fixed in only two geocentric positions depending on the sign of the geocentric velocity of the zero point of the LSR: $v_{\text{geo}}(0_{\text{LSR}})$. This concession allows us to characterize and subtract atmospheric lines—the major source of contamination in our spectra—as accurately as possible. As a result, the actual LSR velocity range (i.e., the endpoints of the **VELOCITY** vector) of pointings varies. For this reason, the integrated release employs the slightly limited range of $\pm 80 \text{ km s}^{-1}$. We chose this option to normalize the range rather than integrating each pointing fully over its velocity vector. As we extend the velocity coverage, we will extend the integration range of the integrated survey releases. The kinematic survey releases contain the full velocity span of each pointing.

For completeness, note that there is a small second order component to the velocity dispersion in WHAM spectra: data points are not spaced equally in velocity. The Δv between data points is close to 2 km s^{-1} but decreases by about 3% from blue to red. In addition, southern survey data points sample a velocity interval $\sim 1.5\%$ larger than northern data due to slight changes in the optical configuration. These effects are not large, but users should use caution when combining or subtracting spectra with large differences in velocity ranges where high precision might be desired. The velocity vectors provided in the full kinematic release (§3.2) retain these characteristics for precision; the FITS kinematic cube (§3.4) regularizes the velocity axis, smoothing the data slightly.

4.2. Intensity

The WHAM intensity calibration is based on a Fabry-Perot calibration of the North American Nebula (NGC 7000) made by Scherb (1981). An estimated correction has been made for the difference in the beam between the instrument used for the calibration and WHAM (50' vs. 60'). Comparison of WHAM survey data with radio (Heiles et al. 2000) and optical data (Gaustad et al. 2001) suggest that our calculated intensity calibration is very good. We conservatively estimate a systematic error of $\pm 10\%$ in our absolute calibration.

Atmospheric extinction curves are calculated for each night where multiple nebular calibration observations were available. An empirically determined, seasonally varying transmission was applied to nights where insufficient data was available. The median zenith transmission at Kitt Peak during the northern survey (1997–1998) was 0.93. To date at CTIO (2009–present) it is 0.92.

Two very minor corrections have also been applied. Very slow degradation in the instrument’s transmission is measurable over its lifetime (1997–present), and a correction has been applied to account for the effect. Finally, a small correction to Kitt Peak data was needed depending on whether a narrow (i.e., geocorona) or broad (i.e., nebular) line source was used to tune the spectrometer prior to survey observations. For southern observations, all tuning is done on broad or white-light sources and this correction is not needed.

4.3. *Atmospheric Lines*

Atmospheric lines are the most significant source of uncertainty in our reduced Galactic emission profiles. In addition to the bright (2–13 R) geocoronal $\text{H}\alpha$ line, numerous fainter (30–150 mR) lines span the entire spectral range. These lines are dense enough that no true ‘flat’ continuum is seen in our spectra at our spectral resolution (10–12 km s^{−1}). In [Hausen et al. \(2002\)](#), we characterize these lines and form an atmospheric template that is subtracted from each spectrum. Each observational block of pointings is combined to form a high S/N (~ 900 –1500 sec) spectrum. We then scale the template to best-fit the faint atmospheric lines in the block-averaged spectra. The parameters from this fit are used to subtract the template from each of the original observations. See [Haffner et al. \(2003\)](#) for more details of this procedure.

The geocoronal line, although smoothly variable among our short exposure observations (30 sec), is well characterized by a single Gaussian at our spectral resolution and is easily fit and removed from all but the brightest Galactic profiles. A small portion of each spectrum has slightly higher noise due to the higher signal of the line that was removed.

4.4. *Zodiacal Light*

As somewhat of a surprise to us, but as a testament to WHAM’s power at detecting faint features, many spectra taken near the beginning or end of the night of the NSS show evidence for a zodiacal absorption feature near $\text{H}\alpha$. Although all observations are taken with the moon set and after astronomical twilight, a residual absorption feature is present after subtracting the geocoronal line from these observations. Most of the feature is hidden by the geocoronal $\text{H}\alpha$ line and is removed with that line in our subtraction procedure. However, a blue- or red-shifted wing of absorption remains near the location of the geocoronal line depending on the look direction of the observation.

Work by Greg Madsen determined that the strength and location of the residual absorption correlates quite well with ecliptic direction and measured distributions of zodiacal light. The radial velocity of the residual also correlates with the orbital velocity of the zodiacal dust along the line of sight. He derived a synthetic absorption profile whose strength was based on this distribution and the direction of an observation. This profile was then subtracted from each spectrum to recover the baseline and any potential Galactic emission. The method does not completely remove the feature in all cases, but it does significantly reduce the systematic residuals (≈ 0.1 R) that were present in our maps. These details are also discussed in [Haffner et al. \(2003\)](#). Aware of this issue when beginning the southern survey, we added zodiacal brightness as a parameter for prioritizing observations to minimize the contribution of the zodiacal spectrum in each pointing.

5. ANOMALIES

5.1. *Missing Pointings*

A survey software bug early in the NSS failed to save the final pointing of a block. Several days of observations were taken before this problem was noticed and fixed. Since then, only very occasional software bugs have caused random missing pointings. The full list of these (32) in the WHAM “bBLOCK_POINTING” notation is here for reference:

b30_49 b31_49 b44_28 b88_49 b174_27 b223_46 b223_47 b223_48
 b223_49 b241_45 b317_42 b369_39 b372_35 b418_34 b420_35
 b428_31 b475_32 b478_27 b484_27 b525_26 b527_27 b528_30
 b533_45 b563_36 b588_43 b603_47 b604_44 b651_42 b705_49
 b714_28 b817_26 b1037_4

In DR1, these pointings have *not* been added into the survey using averages from nearby neighbors as is done with stellar contamination.

5.2. *Offset Pointings*

Three high-latitude ($b < -60^\circ$) blocks (b1169, b1234, and b1201) in DR1 are offset 0.3° – 0.5° from the regular survey grid. This shift was accidentally left in the control software after pointing tests. The data from these nights are still good, but the blocks will appear offset from the normal survey grid pattern. A narrow strip on one side of these blocks has not been captured by the resulting beam pattern. We are hoping to re-observe these blocks in 2017.

5.3. *Velocity Coverage*

With WHAM’s 200 km s^{-1} bandpass, we attempt to cover $v_{\text{LSR}} = \pm 100 \text{ km s}^{-1}$ in a single exposure. This range would capture the bulk of $\text{H}\alpha$ emission from the Milky Way disk aside from some regions near the Galactic plane. However, in order to remove the geocorona with the highest fidelity, we use only two spectral windows for the survey that are fixed in *geocentric* velocity depending on the sign of the geocentric velocity of the zero point of the LSR: $v_{\text{geo}}(0_{\text{LSR}})$ (which varies with location and time throughout the year). This constraint causes variability in the observed LSR velocity window for each pointing.

Due to Galactic rotation, there is also a preference to observe certain regions when $v_{\text{geo}}(0_{\text{LSR}})$ is a particular sign (e.g., observing $\ell \sim 130^\circ - 160^\circ$ with $v_{\text{geo}}(0_{\text{LSR}}) < 0 \text{ km s}^{-1}$ to cleanly capture the Perseus Arm where emission is at $v_{\text{LSR}} < -30 \text{ km s}^{-1}$). With many directions observed only once (to date) for the WHAM-SS, most spectra are not centered around $v_{\text{LSR}} = 0 \text{ km s}^{-1}$. As a result, there is some incompleteness at the high velocities on the red or blue end of most spectra. Since we have kept Galactic rotation in mind when planning observations, little emission is missing even with these current limits. A report of the current coverage for DR1-161116 follows:

3.89% complete at -100 km s^{-1} to $+100 \text{ km s}^{-1}$.
 28.57% complete at -90 km s^{-1} to $+90 \text{ km s}^{-1}$.
 63.10% complete at -80 km s^{-1} to $+80 \text{ km s}^{-1}$.
 1.87% incomplete at $|v| = 60 \text{ km s}^{-1}$.

Some SSS pointings in the first category above have already been observed multiple times during the year near both sign extremes of $v_{\text{geo}}(0_{\text{LSR}})$. More than half of these have velocity coverage between $250\text{--}300 \text{ km s}^{-1}$. The handful of pointings in the last category with the poorest coverage on one end are from SSS observations taken with the wrong spectral window for $v_{\text{geo}}(0_{\text{LSR}})$ that have not yet been re-observed.

6. VERSION HISTORY

6.1. *Data Releases*

DR1-v161116-170111: First public release.

DR1-v161116-170222: Add integrated survey release in FITS image format. Tweak data file header documentation.

DR1-v161116-170317: Add kinematic survey release in FITS cube format. No changes to other formats.

6.2. *Documentation Releases*

01/11/2017: First public release.

02/22/2017: Added description of FITS integrated image release (§3.3) and this section (§6) on version changes.

02/22/2017: Added description of FITS kinematic cube release (§3.4) and tweak some wording in the velocity section (§4.1).

Acknowledgements: The design, construction, and continuing operation of WHAM has been primarily supported by the National Science Foundation. Most recently, the move of the facility to the southern hemisphere and the completion of the all-sky $\text{H}\alpha$ survey were enabled by awards AST-0607512 and AST-1108911. WHAM was built with the additional help of the Wisconsin Graduate School, Physical Sciences Lab, and Space Astronomy Lab. Kurt Jaehnig, Jeff Percival, Sam Gabelt, and Don Michalski have provided essential engineering, technical, and design expertise from the start of the project. The relocation south was made smooth due to the excellent staff at KPNO and CTIO. Without them we would not be able to remotely observe under such fine skies, collecting nearly two decades of fantastic data.

REFERENCES

- Dennison, B., Simonetti, J. H., & Topasna, G. A. 1998, *Publ. Astron. Soc. Australia*, 15, 147
- Finkbeiner, D. P. 2003, *ApJS*, 146, 407
- Gaustad, J. E., McCullough, P. R., Rosing, W., & Van Buren, D. 2001, *PASP*, 113, 1326
- Haffner, L. M., Reynolds, R. J., Tufte, S. L., et al. 2003, *ApJS*, 149, 405
- Haffner, L. M., Reynolds, R. J., Madsen, G. J., et al. 2010, in *Astronomical Society of the Pacific Conference Series*, Vol. 438, *The Dynamic Interstellar Medium: A Celebration of the Canadian Galactic Plane Survey*, ed. R. Kothes, T. L. Landecker, & A. G. Willis, 388
- Haffner, L. M., Reynolds, R. J., Madsen, G. J., et al. 2017, *ApJS*, in prep
- Hausen, N. R., Reynolds, R. J., Haffner, L. M., & Tufte, S. L. 2002, *ApJ*, 565, 1060
- Heiles, C., Haffner, L. M., Reynolds, R. J., & Tufte, S. L. 2000, *ApJ*, 536, 335
- Scherb, F. 1981, *ApJ*, 243, 644